Supplement information

Ultrastructural features between myoblasts using conventional chemical fixation

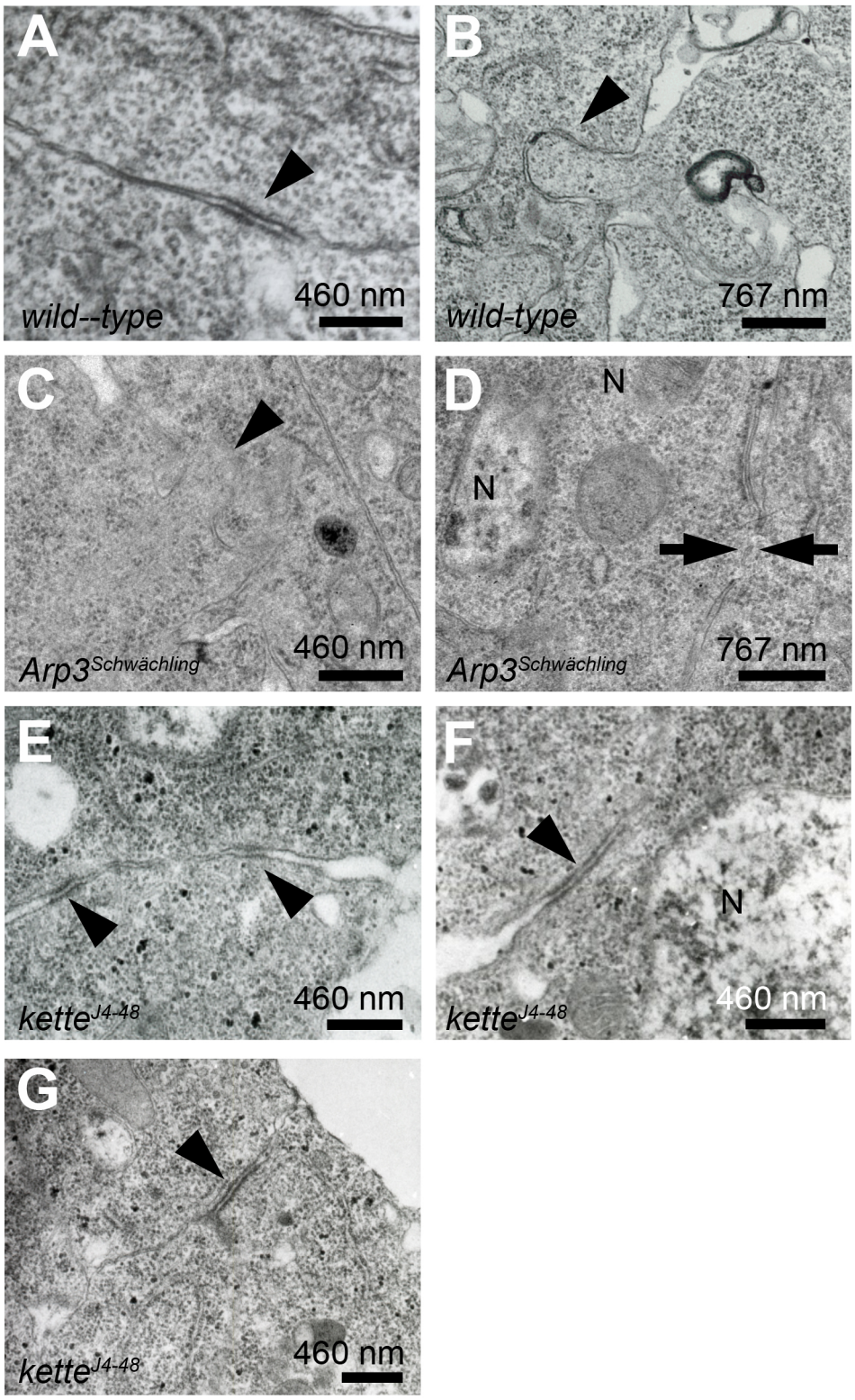

Figure S1 Electron-dense plaques are the most prominent ultrastructural features observed in *kette* mutants.

(A–G) Electron micrographs of stage 14 embryos. Embryos were fixed by using conventional chemical fixation. (A–B) Wild-type myoblasts showing (A) an electron-dense plaque (arrowhead) between adhering myoblasts, and (B) the projection of a finger-like protrusion from one myoblast into the other (arrowhead). In homozygous *Arp3*^{Schwächling} mutants, (C) finger-like protrusions projecting from one myoblast into the other (arrowhead). (D) However, more frequently, a small fusion pore is observed between myoblasts (arrows). (E–G) Homozygous *kette*$^{J4\text{-}48}$ mutants. (E) Two electron-dense plaques that measure 200 nm in length between aligning myoblasts (arrowheads). (F) Electron-dense plaque of 1 μm between adhering myoblasts (arrowhead). (G) Adherence junction between epithelial cells (arrowhead).

Expression of N-cadherin expression in wild-type and *kette* mutant embryos; zygotic abi mutants and embryos expressing Sra1^{Myr}, Sra1ΔC^{Myr} and *wasp*RNAi do not show a myoblast fusion phenotype

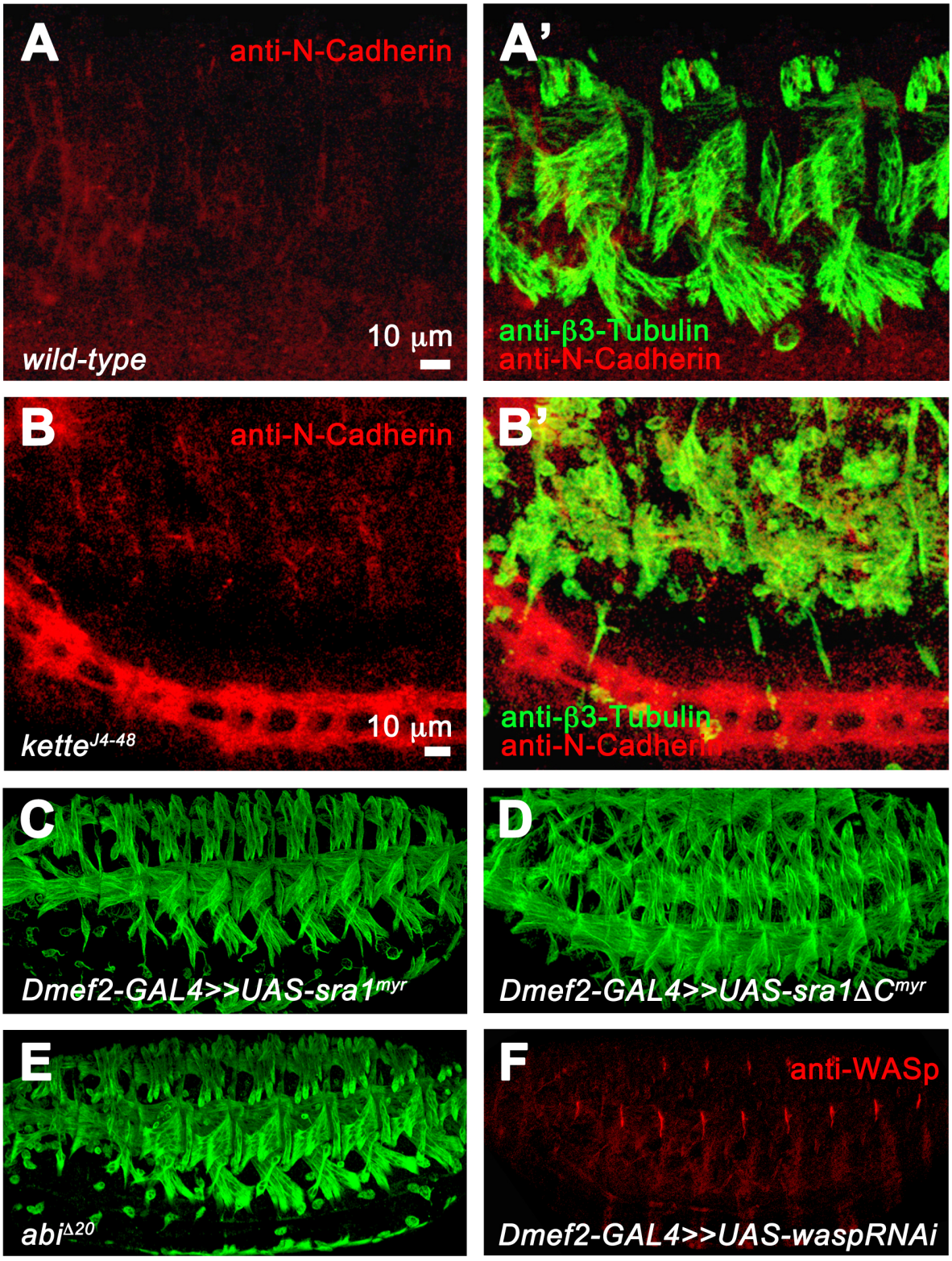

Fig. S2 N-cadherin expression persists in *kette* mutants and Sra1ΔC^{Myr} expressing embryos and *abi* mutants do not show a *kette*-like pehnotype

(A–B') Magnification of stage 16 embryos stained with anti-N-cadherin (red) and anti-β3-Tubulin (green) to visualize myoblasts and mini-muscles. (A, A′) N-cadherin is not detectable at stage 16 in *kette*$^{J4\text{-}48}$/TM3 deformed-lacZ embryos (arrowhead). (B, B′) N-cadherin is present at the membrane of a thin mini-muscle and an unfused myoblast (arrowheads). (C–E) Lateral view of stage 16 embryos stained with anti-β3-Tubulin. (C) Expression of UAS-*sra1*^{myr} and (D) UAS-*sra1*Δ*C*^{myr} in FCs and FCMs. (E) Homozygous *abi*$^{\Delta 20}$ null mutant. (F) Anti-WASp staining of a stage 16 embryo expressing UAS-*waspRNAi* driven by *Dmef2*-GAL4 in FCs and FCMs. WASp is still present in muscles and at attachment sites.

Table S1. Number of embryos and sections analysed by transmission electron microscopy.

Genotype	Number of embryos	Number of electron-dense plaques per section (number of sections)	Length of the electron-dense plaques (number of electron-dense plaques)	Number of finger-like protrusions per section (number of sections)	Number of fusion pores per section (number of sections)
Wild-type	4	4 (20)	500 nm (4)	1 (20)	2 (20)
kette$^{J4\text{-}48}$	4	4 (18)	200 nm (2) 1 µm (2)	0 (18)	0 (20)
scar$^{\Delta 37}$ *vrp*^{f06715}	6	0 (25)	–	0 (25)	3 (25)
Arp3^{Schwächling}	6	1 (25)	200 nm (1)	1 (25)	5 (25)
High-pressure freezing/freeze substitution					
Wild-type	3	0 (12)	–	2 (4)	0 (4)
kette$^{J4\text{-}48}$	2	3 (8)	1 µm (3)	3 (4)	0 (4)